International Journal of Mechanical, Industrial and Aerospace Sciences
ISSN: 2517-9950
Vol:8, No:7, 2014

Comparison on Electrode and Ground Arrangements Effect on Heat Transfer under Electric Force in a Channel and a Cavity Flow

Suwimon Saneewong Na Ayuttaya, Chainarong Chaktranond, Phadungsak Rattanadecho

Abstract**—**This study numerically investigates the effects of Electrohydrodynamic on flow patterns and heat transfer enhancement within a cavity which is on the lower wall of channel. In this simulation, effects of using ground wire and ground plate on the flow patterns are compared. Moreover, the positions of electrode wire respecting with ground are tested in the range of angles $\theta = 0$ - 180^o. High electrical voltage exposes to air is 20 kV. Bulk mean velocity and temperature of inlet air are controlled at 0.1 m/s and 60 ^{O}C, respectively. The result shows when electric field is applied, swirling flow is appeared in the channel. In addition, swirling flow patterns in the main flow of using ground plate are widely spreader than that of using ground wire. Moreover, direction of swirling flow also affects the flow pattern and heat transfer in a cavity. These cause the using ground wire to give the maximum temperature and heat transfer higher than using ground plate. Furthermore, when the angle is at $\theta = 60^o$, high shear flow effect is obtained. This results show high strength of swirling flow and effective heat transfer enhancement.

Keywords**—**Swirling Flow, Heat Transfer, Electrohydrodynamic, Numerical Analysis.

I. Introduction

HEAT transfer enhancement is the one of the most important application subjects of the thermal engineering field which increases the effectiveness of the drying process as well as significant technical advantages and savings energy consumption. By promoting higher convective heat transfer coefficient, the enhancement techniques are divided into two groups so called active and passive techniques. In which the electrohydrodynamic (EHD) phenomenon is an active method and deals with the interactions between electric field, flow field and temperature field. The main advantage of electrohydrodynamic is that it directly converts electrical energy into kinetic energy without mechanical pieces. Moreover, the influence of electrohydrodynamic phenomena can change the pattern of airflow and enhances transport phenomena with lowering energy supplied. When electrical high voltage is applied to the tip of electrode, air in its vicinity is ionized and the ion is moved to the ground [1]. Therefore, ionized air moves from the electrode to the ground and conducts the shear flow caused by the difference in air velocity between charged and uncharged airflows. Consequently, the shear flow induces a swirling flow [2].

Previous studies, many researchers have studied the electrohydrodynamic for heat transfer enhancement [3]-[6]. Go et al. [5] experimentally studied enhancement of forced convection heat transfer using an ionic wind. Little variation of the ionic wind heat transfer coefficient with the heat flux imposed on the ground plate was observed, which suggested that the electrohydrodynamic interaction was due to largely hydrodynamic effects rather than electrically induced thermal effects. Experiments with different electrode gaps reveal slight changes in both upstream and downstream enhancement but consistency in terms of the location of maximum enhancement near the corona wire. Huang and Lai [6] numerically studied the water evaporation enhanced by corona wind. The results showed that water evaporation could be greatly enhanced by corona wind. However, a cross-flow with a high velocity may diminish the effect of corona wind. The numerical results were also compared with experimental data reported in the literature. A satisfactory agreement was found between these results.

The high electrical voltage is applied at the tip of electrode and air is moved to the ground so flow pattern characteristics are depend on ground types. From the past decades, two types of ground arrangement are studied. The first and the second types are wire and plate groups, respectively. Zhao and Adamiak [7] numerically studied electric field and flow field of various Reynolds number (Re) by using plate ground arrangement. It was found that at very low Re (<15), the EHD flow was dominated in the channel when Re increased; the significance of the EHD wakes gradually decreases. Ramachandran and Lai [8] experimentally studied effects of porosity on the performance of EHD-enhanced drying by using ground plate arrangement. Comparison with solid glass beads of various sizes were evaluated the dependence between the material structure (in terms of its porosity) and the effectiveness of corona wind in drying. The results showed that effect of porosity in the drying enhancement by corona wind. The drying enhancement of 5 mm perforated beads in some cases may exceed than 6 mm solid beads because the hole in a 5 mm perforated bed was straight through its center, the moisture path in 5 mm perforated beads may be more restricted than that of 6 mm solid beads. Chaktranond and Rattanadecho [9] experimentally studied the heat and mass transfer enhancement in porous material subjected to electric field using ground wire. The results showed that the

Suwimon Saneewong Na Ayuttaya is with the Chulachomklao Royal Military Academy, Nakhon-Nayok, 26001 Thailand (corresponding author to provide phone: +66 37 393 487; fax: +66 37 393 487; e-mail: joysuwimon1@hotmail.com).

Chainarong Chaktranond and Phadungsak Rattanadecho are with the Thammasat University (Rangsit Campus), Pathumthani 12120 Thailand (e-mail: cchainar@engr.tu.ac.th, ratphadu@engr.tu.ac.th).

convective heat transfer coefficient and drying rate were considerably enhanced with the strength of electric field influencing Corona wind. Saneewong Na Ayuttaya et al. [10] numerically explored the influences of electrode arrangements and the number of electrodes on the swirling flow under electric field. The result showed that the distance between electrode and ground wire in the horizontal direction become closer, size of swirling becomes smaller but vorticity is stronger. This is because of higher and denser electric field intensity. With increasing the number of electrodes, electric field increased. This causes swirling flow to be larger and more violent.

By comparing flow visualization, simulation results had good agreement with experiments. There are few studies on the effect of electrode and ground arrangements on heat transfer under electric force. In this current study, electrode arrangement and both of types (ground wire and ground plate) are compared. By behavior of flow pattern direction in a cavity flow are investigated in order to clearly consider flow characteristic with and without electrohydrodynamic effect.

II. Numerical Modeling

The illustration of computational domain and boundary conditions as shown in Fig. 1. The dimension comprise of main three parts: (1) electric field (2) fluid flow and (3) heat transfer. Dimensions of a channel flow are 2.0 m (long) × 0.3 m (high) and it is filled with air at 60°C. A cavity of 10 cm × 5 cm is placed at the lower wall and it is filled with air at 20°C. Space charge density (q_0) at the tip of electrode is considered from David [11]. Electrode and ground wire are assumed to be a circle with a diameter of 0.5 mm. Position of ground wire is fixed at x = 0, y = 0. Ground plate is stalled above cavity and 4 cm (long), position of ground plate is fixed at x = 0. The distance between electrode and ground (d) is fixed at 4 cm.

Electric force calculations refer to (1) to (4). To simplify the problem, the dielectric property is constant and the effect of magnetic field is negligible. Electric field distribution is computed from Maxwell's equations listed as below:

$$\nabla \cdot \varepsilon \vec{E} = q \tag{1}$$

$$\vec{E} = -\nabla V \tag{2}$$

$$\nabla \cdot J + \frac{\partial q}{\partial t} = 0 \tag{3}$$

$$J = qb\vec{E} + q\vec{u} \tag{4}$$

where E is electric field, t is time, q is the space charge density in the fluid, ε is dielectric permittivity, V is electrical voltage, J is current density, b is ion mobility and u is airflow velocity. When electrical voltage of wire (V_0) is considered, it is fixed at V_0 = 20 kV. Electric force is computed by Coulomb force as shown in (5),

$$\vec{F}_E = q\vec{E} \tag{5}$$

Fluid flow calculation refers to (6), the inlet air velocity is uniform and u_i = 0.1 m/s. Properties of fluids are assumed to be constant and evaporation effect is neglect. Fluid flow is computed through the continuity and Navier–Stokes equations, where electric force is included,

$$\rho\left[\frac{\partial \vec{u}}{\partial t} + (\vec{u}\cdot\nabla)\vec{u}\right] = -\nabla\vec{P} + \mu\nabla^2\vec{u} + \vec{F}_E \tag{6}$$

where P is pressure, ρ is density of fluid and μ is viscosity of fluid. The last term of (6) is electric force per unit volume. Enhancement of airflow velocity is presented by velocity ratio (u_r), which is defined as the maximum velocity perturbed by electric field ($u_{max,EHD}$) to inlet airflow velocity (u_i) as shown (7),

$$u_r = \frac{u_{max,EHD}}{u_i} \tag{7}$$

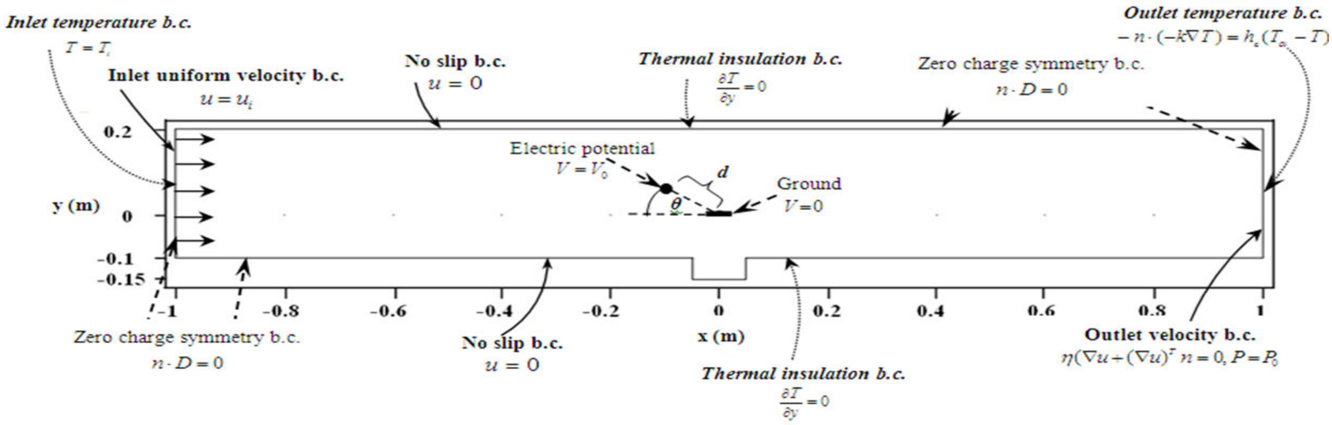

Fig. 1 Air flowing through a channel and a cavity with electrode and ground arrangement

From heat transfer calculation, effect of Joule heating is neglected and emission or absorption of radiant energy is not considered. Temperature distribution in a channel flow is calculated by energy equation as refer to (8),

$$\rho C_p\left[\frac{\partial T}{\partial t}+\vec{u}\nabla T\right]=k\left(\nabla^2 T\right) \tag{8}$$

where C_p is the specific heat capacity and k is thermal conductivity and T is temperature. The initial temperature of hot-airflow in channel is be $T(t_0)$ = 60 °C. Convective heat transfer coefficient (h) is defined by the thermal equilibrium as refer to (9),

$$h=-\frac{k_c}{\Delta T}\frac{\partial T}{\partial n} \tag{9}$$

where n is normal vector and k_c is thermal conductivity of a cavity. The initial temperature of a cavity is $T_c(t_0)$ = 20 °C. Enhancement of heat transfer is presented by average convective heat transfer ratio (h_r) which is the ratio of average convective heat transfer coefficient perturbed by electric field ($\overline{h}_{EHD}$) to average convective heat transfer of free air ($\overline{h}_{free\ air}$) as refer to (10),

$$h_r=\frac{\overline{h}_{EHD}}{\overline{h}_{free\ air}} \tag{10}$$

The properties of air and cavity are shown in Tables I and II, respectively.

TABLE I
PROPERTIES OF AIR

Symbol	Modeling Parameter	Value
b	Ion Mobility	1.80×10^{-4} m²/V.s
ε	Dielectric Permittivity	8.85×10^{-12} F/m
η	Kinematics Viscosity	1.76×10^{-5} m²/s
ρ	Density	1.060 kg/m³
C_p	Specific Heat Capacity	1.008 kJ/kg.K
k	Thermal Conductivity	0.028 W/m.K

TABLE II
PROPERTIES OF CAVITY

Symbol	Modeling Parameter	Value
η_c	Kinematics Viscosity	1.50×10^{-5} m²/s
ρ_c	Density	1.177 kg/m³
C_{pc}	Specific Heat Capacity	1.005 kJ/kg.K
k_c	Thermal Conductivity	0.50261 W/m.K

This study employs the commercial software, COMSOL, to solve the governing equations. The Coulomb force is computed from Maxwell's equations. Air is assumed to be incompressible flow and is computed from the continuity and Navier-Stokes equations. Simultaneously, energy equation is used to investigate the temperature of airflow. With finite element method, this convergence test leads to the mesh with approximately 13,000 elements. It is reasonable to assume that, with this element number, the accuracy of the simulation results is independent on the number of elements and therefore save computation memory and time. Higher numbers of elements are not tested due to lack of computational memory and performance.

III. Results and Discussion

In this numerical analysis show the effects of electrode positions and ground types on flow patterns and enhancement of heat transfer in a cavity. Electrode positions respecting with ground position is varied in the range of θ = 0 to 180°, as well as, ground types are wire and plate.

A. Comparison on with and without Effect on Inlet Airflow under Electric Force

Flow pattern is compared both of within a channel and a cavity flow when various inlet airflow velocity.

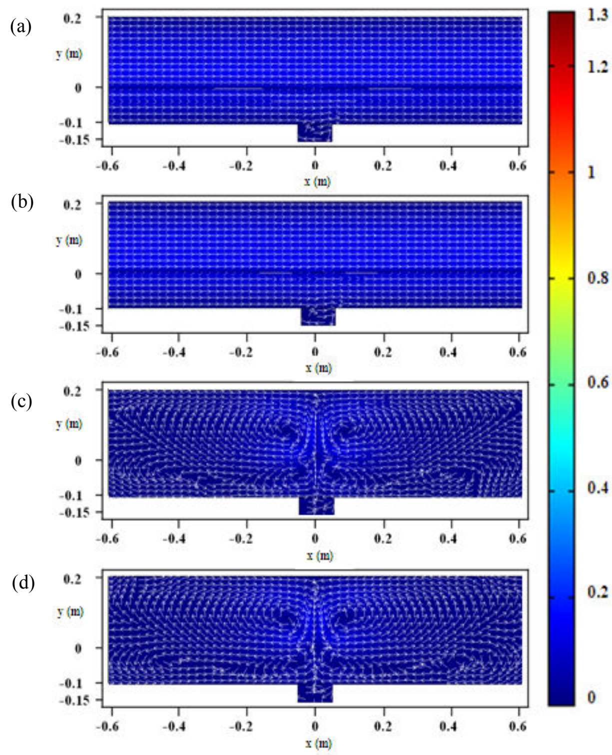

Fig. 2 Swirling flow in various inlet airflow velocity (a) ground wire, with u_i = 0.1 m/s and no EHD effect (b) ground plate, u_i = 0.1 m/s and no EHD effect (c) ground wire, u_i = 0 m/s, EHD effect and θ = 90° (d) ground plate, u_i = 0 m/s, EHD effect and θ = 90° when consider within a channel flow

Fig. 2 shows flow pattern within a channel flow when no EHD and EHD effect (θ = 90°) are investigated from Figs. 2 (a), (b) and Figs. 2 (c), (d), respectively. The swirling flow is not presented in case of No EHD but it is presented when consider the EHD effect. With EHD effects and no inlet airflow velocity, swirling flow is appeared both of ground wire (Fig. 2 (c)) and ground plate (Fig. 2 (d)). With using ground plate, swirling flow is widely spreader than ground wire. This causes airflow within a cavity to spread over as shown in Fig. 3. By No EHD (Fig. 3 (a), (b)), recirculation of airflow within a cavity flow is appeared. By EHD case, airflow within a cavity is induced by swirling flow. It can be seen that airflow within a cavity from ground plate (Fig. 3 (d)) is more spreader than ground wire (Fig. 3 (c)). From the data, in case of no inlet airflow velocity, airflow velocity within a channel flow is increased by swirling flow effect so shear flow effect can increase the airflow within a cavity flow.

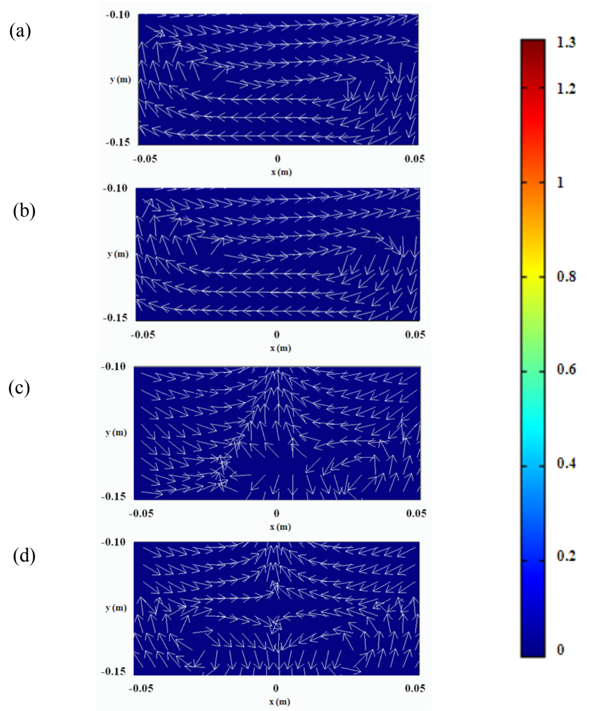

Fig. 3 Swirling flow in various inlet airflow velocity (a) ground wire, with $u_i = 0.1$ m/s and no EHD effect (b) ground plate, $u_i = 0.1$ m/s and no EHD effect (c) ground wire, $u_i = 0$ m/s, EHD effect and $\theta = 90^o$ (d) ground plate, $u_i = 0$ m/s, EHD effect and $\theta = 90^o$ when consider within a cavity flow

B. Comparison on Electrode and Ground Arrangements Effect on Swirling Flow under electric Force

Effects of electrode positions and ground types (wire and plate) are shown in Figs. 4 and 6, the swirling flow patterns are similar when consider in each angle of electrode (θ). High electrical voltage exposes to air is 20 kV and bulk mean velocity of inlet air is controlled at 0.1 m/s. It can be seen that placing the electrode with different angles obtains the different flow patterns. This is because electrode force induces shear flow effect in different directions, resulting in different characteristics of swirling flow. Fig. 4 shows results obtaining from ground wire. Swirling flow is clearly seen when the angle $\theta = 0 - 120^o$. This is because electric force is strong enough to construct shear flow layer. With highly swirling flow, airflow is stronger to circulate in a cavity. When $\theta = 60^o$ (Figs. 4 (b) and 6 (b)), it gives the maximum strength of swirling, resulting in enhancement of air velocity. With inlet airflow is moved from the left to the right direction, airflow within a channel flow from EHD cases is supported with airflow direction so maximum velocity field is greatly increased. Fig. 5 shows airflow within a cavity flow, it can be seen that swirling flow direction within a channel flow is related with airflow within a cavity flow. Furthermore, strength of swirling flow in each case is influenced within a cavity flow. Swirling flow in case of $\theta = 60^o$ is the mostly supported by inlet airflow so the maximum airflow within a cavity for is appeared in this case. By inlet airflow is the primary flow and electric filed moves from electrode to ground in order to induce the shear flow or secondary flow. Moreover, influences the characteristic and direction of flow patterns are depended on shear flow direction.

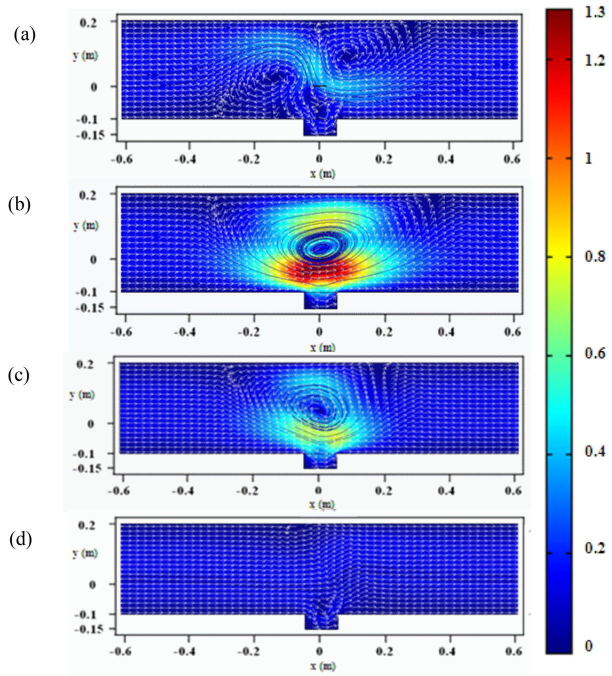

Fig. 4 Swirling flow of ground wire in various θ: (a) $\theta = 0^o$ (b) $\theta = 60^o$ (c) $\theta = 120^o$ and (d) $\theta = 180^o$ when consider within a channel flow and $u_i = 0.1$ m/s

With ground wire arrangement (Fig. 4) is compared with ground plate arrangement (Fig. 6), the swirling flow patterns are similar when consider in each angle of electrode (θ). The flow patterns obtained from using ground wire and plate types are not much different. With using ground plate, swirling is widely spreader. This causes airflow within a cavity to spread over the upper part of cavity, as shown in Fig. 7.

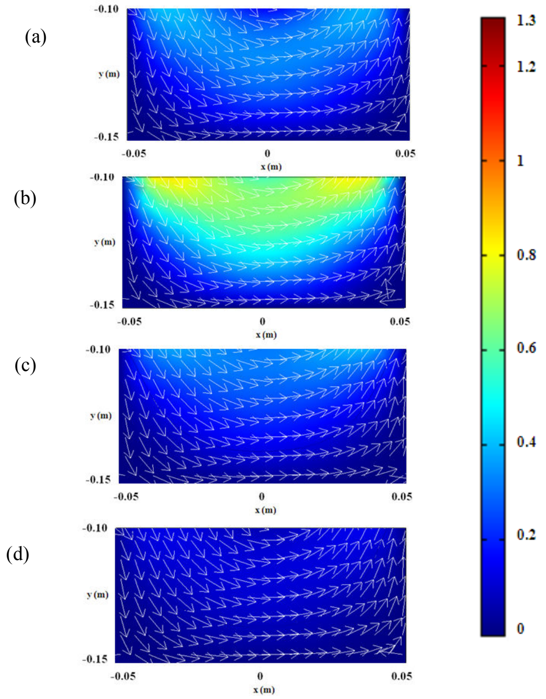

Fig. 5 Airflow of ground wire in various θ: (a) $\theta = 0^o$ (b) $\theta = 60^o$ (c) $\theta = 120^o$ and (d) $\theta = 180^o$ when consider within a channel flow and $u_i = 0.1$ m/s

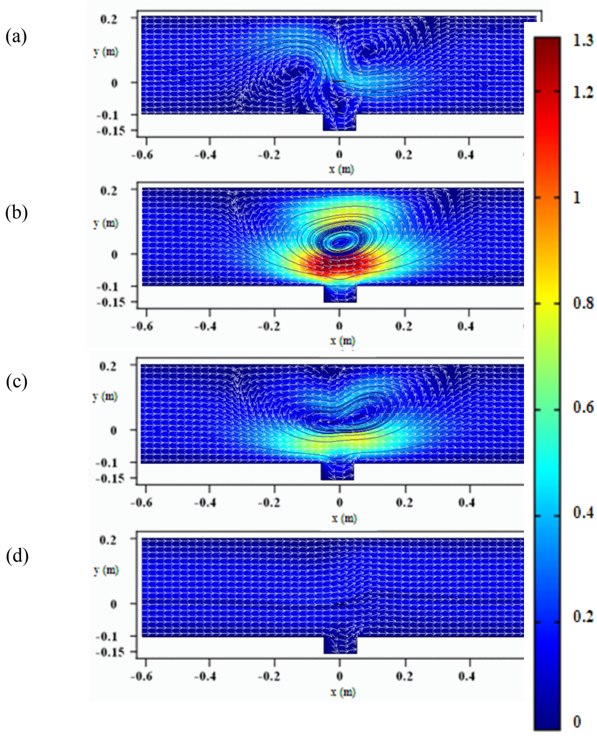

Fig. 6 Swirling flow of ground plate in various θ. (a) $\theta = 0^o$ (b) $\theta = 60^o$ (c) $\theta = 120^o$ and (d) $\theta = 180^o$ when consider within a channel flow and $u_i = 0.1$ m/s

In addition, the maximum velocity ratio and the average velocity ratio from ground wire are higher than that from ground plate. Although, airflow is appeared both of a channel and a cavity flow but initial temperature is differenced so surface tension or interface area between a channel and a cavity flow is considered. With various each angle of electrode and ground type, the maximum velocity ratio (Fig. 8) in each case is little differences when comparing with the average velocity of x-axis between interface areas (Fig. 9). From above data, in the all cases, the maximum velocity ratio and the average velocity 0f x-axis between interface areas of ground wire arrangement are more than that of ground plate arrangement.

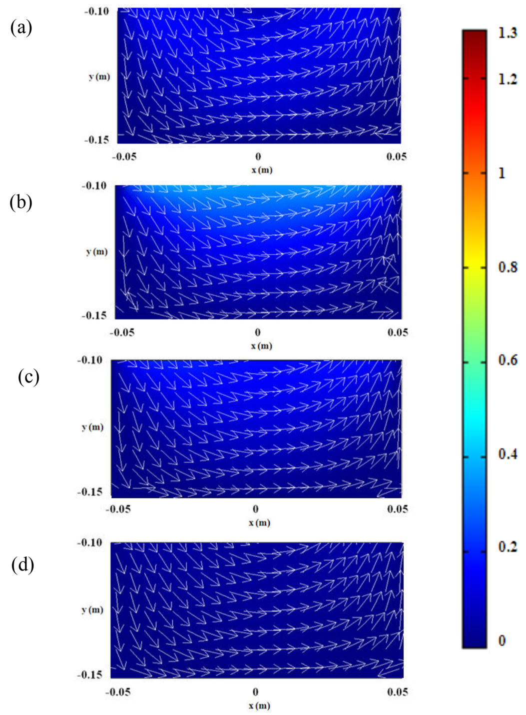

Fig. 7 Airflow patterns of ground plate in various θ: (a) $\theta = 0^o$ (b) $\theta = 60^o$ (c) $\theta = 120^o$ and (d) $\theta = 180^o$ when consider within a channel flow and $u_i = 0.1$ m/s

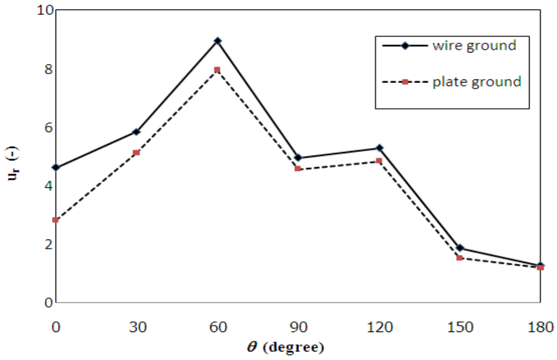

Fig. 8 The maximum velocity ratio (u_r) in various θ and ground type

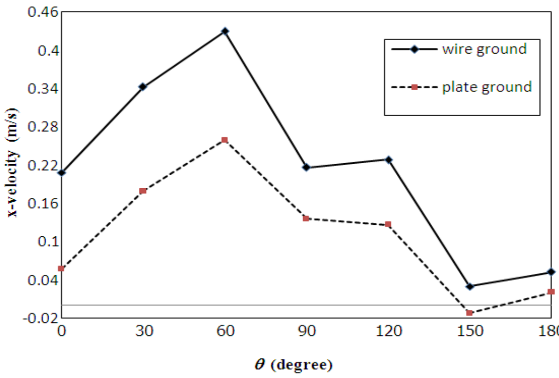

Fig. 9 The average velocity x-axis between interface areas in various θ and ground type

C. Comparison on with and without Effect on Temperature Distribution under Electric Force

Temperature distribution is compared both of within a channel and a cavity flow when various inlet airflow velocity.

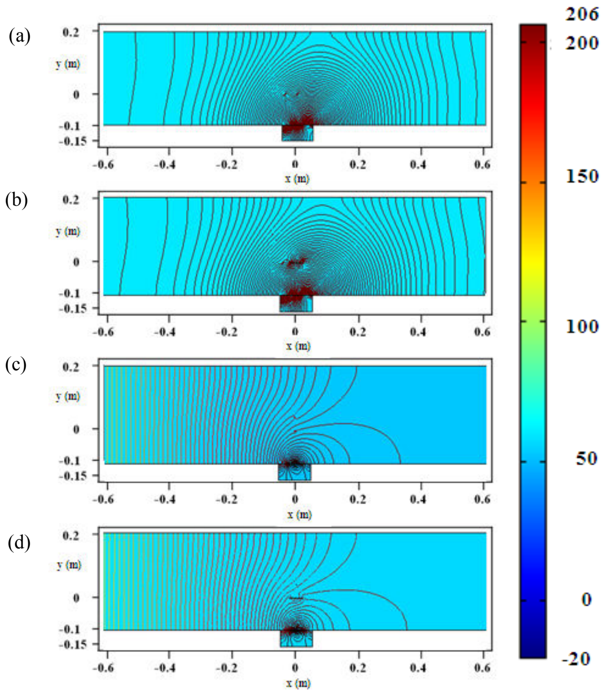

Fig. 10 Temperature contour in various inlet airflow velocity (a) ground wire, with $u_i = 0.1$ m/s and no EHD effect (b) ground plate, $u_i = 0.1$ m/s and no EHD effect (c) ground wire, $u_i = 0$ m/s, EHD effect and $\theta = 90^o$ (d) ground plate, $u_i = 0$ m/s, EHD effect and $\theta = 90^o$ when consider within a cavity flow

Fig. 10 shows temperature contour within a channel flow when no EHD and EHD effect ($\theta = 90^o$) are investigated from Figs. 10 (a), (b) and (c), (d), respectively. With effect of swirling flow near the upper wall as shown in Figs. 10 (c), (d), heat is much transferred from primary flow into the lower wall. It causes temperature of sample to be increased faster, and temperature of air at downstream to be lower. Temperature contour within a cavity is showed in Fig. 11, by the swirling flow is presented when consider the EHD effect so temperature distribution is transferred through a cavity flow as shown in Figs. 11 (c), (d).

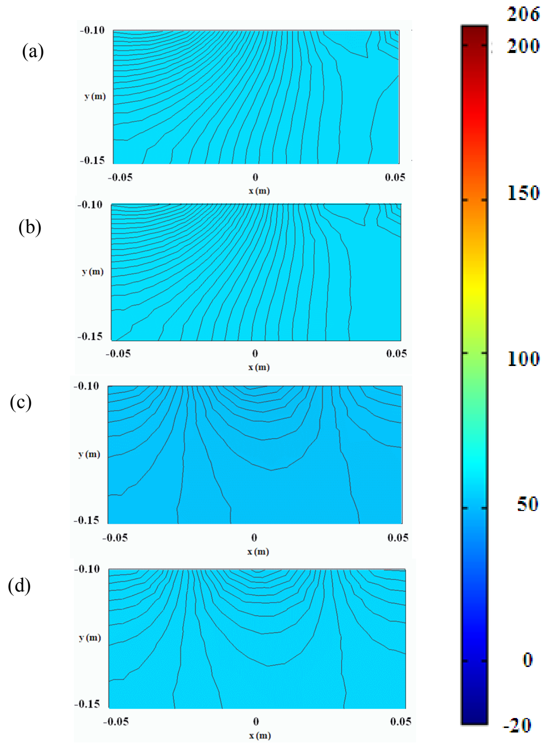

Fig. 11 Temperature contour in various inlet airflow velocity (a) ground wire, $u_i = 0.1$ m/s and no EHD effect (b) ground plate, $u_i = 0.1$ m/s and no EHD effect (c) ground wire, $u_i = 0$ m/s, EHD effect and $\theta = 90^o$ (d) ground plate, $u_i = 0$ m/s, EHD effect and $\theta = 90^o$ when consider within a cavity flow

D. Comparison on Electrode and Ground Arrangements Effect on Heat Transfer under Electric Force

High electrical voltage exposes to air is 20 kV. Bulk mean velocity and temperature of inlet air are controlled at 0.1 m/s and 60°C, respectively. Figs. 12 and 13 show the effect of ground types on temperature distribution in various θ at $t = 60$ sec. It can be seen that temperature distribution in a channel depends on characteristics of swirling flow. The temperature from using ground plate (Fig. 13) distributes more than that from using ground wire (Fig. 12). The maximum temperature of wire cases is more than that of ground plate cases. Furthermore, trend of temperature distribution is resembled with the average velocity of x-axis between interface areas (Fig. 9). The average convective heat transfer ratio between interface areas (Fig. 14) is related with the maximum temperature ratio within a cavity flow and the average velocity of x-axis between interface areas.

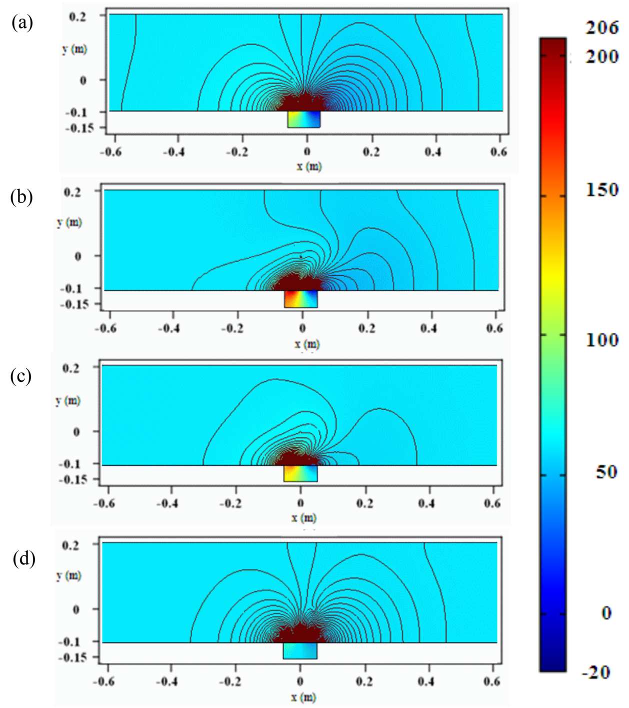

Fig. 12 Temperature contour in a channel from using ground wire in various θ when t = 60 sec: (a) $\theta = 0^o$ (b) $\theta = 60^o$ (c) $\theta = 120^o$ and (d) $\theta = 180^o$

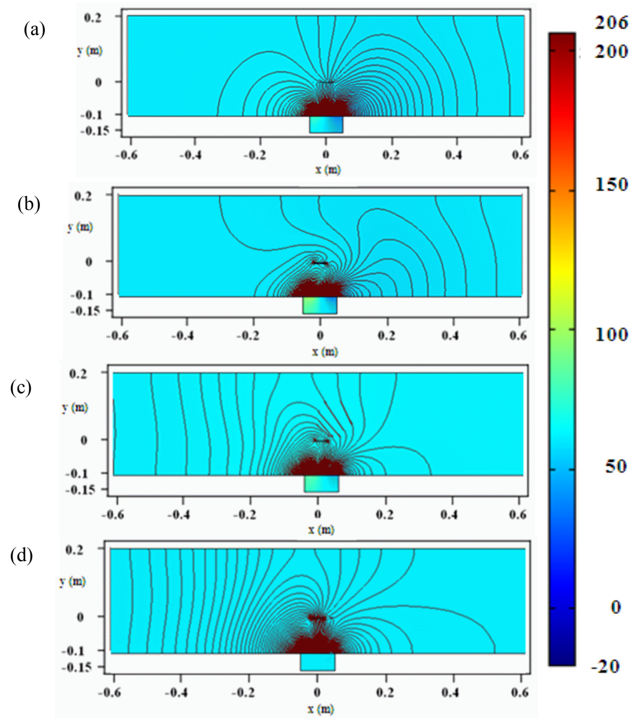

Fig. 13 Temperature contour in a channel from using ground plate in various θ when t = 60 sec: (a) $\theta = 0^o$ (b) $\theta = 60^o$ (c) $\theta = 120^o$ and (d) $\theta = 180^o$

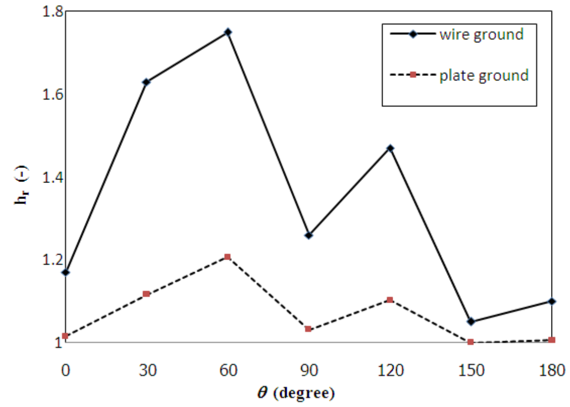

Fig. 14 The average convective heat transfer ratio between interface areas in various θ and ground type when t = 60 sec

From above data it can be seen that ground wire and plate ground arrangements are properly installed for locally and widely swirling flow for drying process, respectively. Finally, the convective heat transfer is depended on the average velocity of x-axis between interface areas. It means that induction of airflow within a cavity flow is more influenced than the strength of airflow in a channel flow.

IV. Conclusion

The swirling flow pattern and temperature distribution due to EHD-enhanced convective heat transfer within a channel flow are numerically studied and the following conclusions can be highlighted:

1. With the effect of angle between electrode and ground, shear flow from electric force is induced the difference direction so swirling flow is appeared the difference of flow pattern.
2. The strength of swirling flow and temperature distribution of ground wire arrangements are more than that of ground plate arrangement due to difference of airflow induction.
3. Within a channel flow, swirling flow and temperature distribution from ground plate arrangements are widely spreader than ground wire arrangements so airflow within a cavity flow in case of plate ground is spreader over the interface between a channel flow and a cavity flow.

Acknowledgment

Suwimon Saneewong Na Ayuttaya wishes to express their deepest gratitude to the Thailand Research Fund (TRF) for the financial support of this project.

References

[1] H. M. Deylami, N. Amanifred, F. Dolati, R. Kouhikamali, and K. Mostajiri, "Numerical investigation of using various electrode arrangements for amplifying the EHD enhanced heat transfer in a smooth channel," J.Electrostatics, vol. 71, pp. 656-665, March 2013.
[2] S. Saneewong Na Ayuttaya, C. Chaktranond, P. Rattanadecho, and T. Kreewatcharin, "Effect of Ground Arrangements on Swirling Flow in a Channel Subjected to Electrohydrodynamic Effects," ASME J. Fluids Eng, vol. 134, pp. 051211-1-051211-10, March 2012.

[3] J. Seyed-Yagoobi, and J.E. Bryan, “Enhancement of Heat Transfer and Mass Transport in Single-Phase and Two-Phase Flows with Electrodynamics,” Adv. In Heat Transfer, vol. 33, pp. 95-186, April 1999.
[4] S.D. Oh, and H.Y. Kwak, “Electrohydrodynamic (EHD) Enhancement of Boiling Heat Transfer of R113+WT4% Ethanol,” J. Mech. Sci. and Tech, vol. 20, pp. 681-691, March 2006.
[5] D.B. Go, R.A. Maturana, T.S. Fisher, and S.V. Garimella, “Enhancement of external forced convection by ionic wind,” Int.J.Heat and Mass Transfer, vol. 51, pp. 6047-6053, July 2008.
[6] M. Huang, and F.C. Lai, “Numerical study of EHD-enhanced water evaporation,” J.Electrostatics, vol. 68, pp. 364-370, August 2010.
[7] L. Zhao, and K. Adamiak, “Numerical Simulation of the Electrohydrodynamic Flow in a Single Wire-Plate Electrostatic Precipitator,” IEEE Trans. Ind. Appl, vol. 44(3), pp. 683-691, May/June 2008.
[8] M. R. Ramachandran, and F. C. Lai, “Effects of Porosity on the EHD-Enhanced Drying,” Drying Technol, vol. 28, pp. 1477-1483, November 2010.
[9] C. Chaktranond and P. Ratanadecho, “Analysis of heat and mass transfer enhancement in porous material subjected to electric fields (effects of particle sizes and layered arrangement),” Exp. Therm. Fluid Sci, vol. 34, pp. 1049-1056, February 2010.
[10] S. Saneewong Na Ayuttaya, C. Chaktranond, and P. Rattanadecho, “Numerical Analysis of Influence of Electrode Position on Fluid Flow in 2-D Rectangular Duct Flow,” J. Mech. Sci. and Tech, vol. 207(7), pp. 1957-1962, March 2013.
[11] J. G. David, “Introduction to Electrohydrodynamics,” in Plastics, 3rd ed. New Jersey: Prentice Hall International, 1999, pp.123-125.